

1 This document is the Accepted Manuscript version of a
2 Published Work that appeared in final form in the
3 *Canadian Journal of Chemistry*, copyright © Canadian
4 Science Publishing, after peer review and technical
5 editing by the publisher.

6
7 To access the final edited and published work see

8
9 *Can. J. Chem.* **2023**, *101*, 12, 892-902

10
11 [https://cdnsciencepub.com/doi/full/10.1139/cjc-2022-](https://cdnsciencepub.com/doi/full/10.1139/cjc-2022-0314)
12 [0314](https://cdnsciencepub.com/doi/full/10.1139/cjc-2022-0314)

13

14

When is a Pyridine Not a Pyridine?

15

Benzannulated *N*-Heterocyclic Ligands in

16

Molecular Materials Chemistry

17

18

David E. Herbert*

19

20

21

Department of Chemistry and the Manitoba Institute for Materials, University of Manitoba, 144

22

Dysart Road, Winnipeg, Manitoba, R3T 2N2, Canada

23

24

*david.herbert@umanitoba.ca

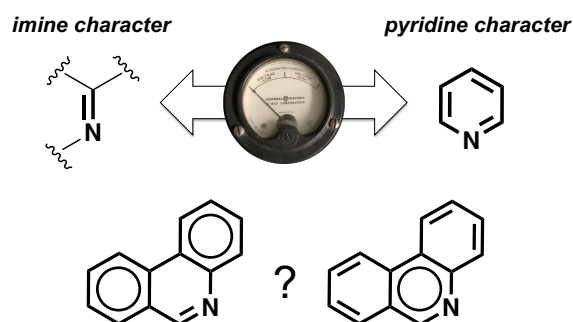
25 ABSTRACT

26 The C=N bond is a critical structural piece of many *N*-donor ligand scaffolds and is central to the
27 properties and reactivity of important coordination complexes. For example, C=N units play a key
28 role in the ‘redox non-innocence’ of α -diimine complexes and in making charge-transfer excited-
29 state character available to complexes of *N*-heterocyclic ligands such as bipyridine. In *N*-
30 heterocycles like pyridine, benzannulation can be used to extend the conjugated C=N containing
31 π -system to quinoline (2,3-benzopyridine) to acridine (2,3-benzoquinoline). This stabilizes the
32 lowest unoccupied molecular orbital (LUMO) of the molecule and boosts its electron-accepting
33 properties, but the position of the benzannulation matters. For example, phenanthridine (3,4-
34 benzoquinoline), an asymmetric isomer of acridine, bears a similarly electronically accessible
35 extended π -system but with a more chemically isolated ‘imine-like’ C=N moiety. This Award
36 Paper presents an overview of our work investigating the impact of such site-selective
37 benzannulation on the chemistry and properties of phenanthridine as a molecule and ligand.

38 Keywords

39 ligand design, coordination chemistry, photophysics, molecular materials

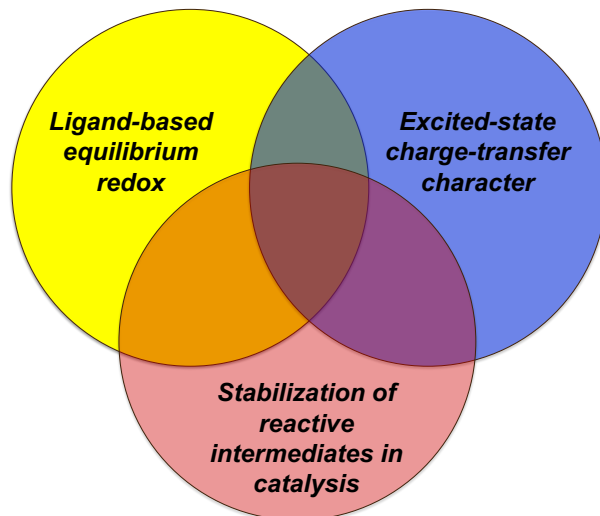
40 Table of Contents Graphic



42 INTRODUCTION

43 Given the myriad applications of coordination complexes from homogenous catalysis to
44 luminescent emitters, a detailed understanding of how molecular properties can be tuned through
45 ligand design can be profitable in many ways.¹ Purposefully designed ligands have enabled, *inter*
46 *alia*, the discovery of base metal hydrogenation catalysts,²⁻⁴ sustainable-element emissive
47 molecules,⁵ and anolyte candidates for redox-flow batteries,⁶ demonstrating the reach of ligand
48 design to impact areas from synthesis to molecular materials chemistry to energy science. Ideally,
49 a particular ligand framework would demonstrate wide versatility and be useful in imbuing
50 reactivity and properties relevant to a variety of settings. Such an approach borrows from the
51 concepts of ‘privileged structures’⁷ in medicinal chemistry – the discovery that particular
52 biological ligands can bind a diverse library of receptors – and ‘privileged catalysts’⁸ in chiral
53 catalysis – narrow classes of synthetic catalysts which can achieve enantioselective reactivity in a
54 wide range of different reactions – and extend these ideas to electronic properties and the activation
55 of small molecules. In thinking of a role for ligand design in these contexts, it might be noted that
56 boundary-pushing ideas such as ligand ‘redox non-innocence’⁹ and ‘metal-ligand cooperativity’¹⁰
57 (‘chemical non-innocence’) both exploit ligand character in the frontier orbitals of a coordination
58 complex. Similarly, the useful photoredox of prototypical sensitizers such as ruthenium(II)
59 *tris*(2,2'-bipyridine) ($[\text{Ru}^{\text{II}}(\text{bpy})_3]^{2+}$) is derived from ligand participation in forming long-lived
60 metal-to-ligand charge-transfer (MLCT) excited states.¹¹ This raises a question: can common
61 molecular features be identified that could in one context favour ligand-based equilibrium redox,
62 while in another confer charge-transfer character to excited-states, and in yet another help stabilize
63 reactive intermediates in catalysis (Figure 1)?

64

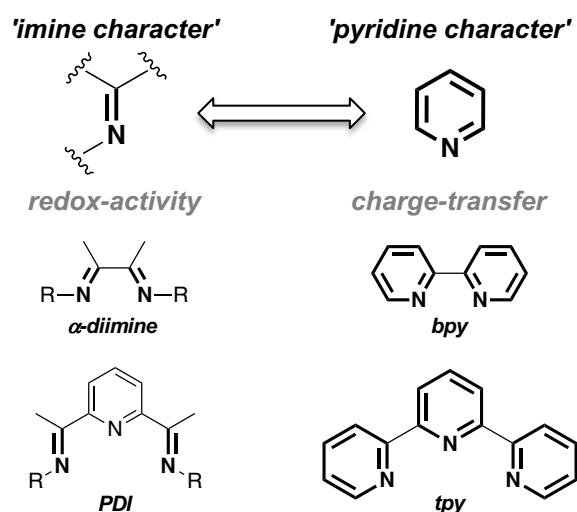


65
 66 **Figure 1.** Seeking commonalities in ligand designs in pursuit of ‘privileged ligand scaffolds’ for
 67 applications of coordination complexes in organometallic chemistry.

68
 69 C=N units appear ubiquitously in ligands whose complexes exhibit a wide range of exciting
 70 reactivity that makes use of both strong Lewis basic nitrogen coordination to metals and the
 71 presence of energetically accessible, vacant π^* orbitals. Such ligands include C=N units as isolated
 72 imines, prominent examples of which include α -diimines¹² and pyridyldiimines¹³ (PDIs), and as
 73 part of delocalized *N*-heterocycles such as 2,2'-bipyridine (bpy) and 2,2':6',2''-terpyridine (tpy;
 74 Figure 2).¹⁴ The vacant, localized C=N π^* orbitals of imine-based ligands like PDIs can be
 75 exploited to access ligand-centred redox in transition metal¹⁵ and main-group complexes.¹⁶ For
 76 example, (PDI)Fe(L) (L = N₂, NH₃) complexes contain ligand-centered triplet PDI diradical
 77 dianions antiferromagnetically coupled to ferrous iron centres, not neutral closed-shell singlet
 78 PDIs bound to Fe(0).¹⁷ PDI ligands can thus serve as ‘electron reservoirs’, storing reducing
 79 equivalents which may then be used profitably in chemical reactions. For example, oxidative
 80 addition of halogens to U(IV) complexes bearing triply reduced [PDI]³⁻ units has been shown to
 81 occur without a change to the metal oxidation state.¹⁸ Similarly, pseudo-octahedral bis(PDI)
 82 complexes of Fe(II) present two PDI-based ligand reductions at accessible potentials.¹⁹ A range of

83 [(PDI)₂Fe]²⁺ complexes can be prepared with *N*-aryl rings containing both electron-releasing and
 84 electron-withdrawing substituents at the *para*-positions through direct condensation of substituted
 85 anilines with 2,6-diacetylpyridine (for electron-releasing substituents)^{19,20} or via Zn-templated
 86 proligand synthesis for electron-withdrawing anilines.²¹ Controlled potential electrolysis
 87 experiments show the reduced species are: (a) as soluble as the dications in organic solvents such
 88 as acetonitrile; (b) relatively stable over extended cycling with high Coulombic efficiencies;²⁰ and
 89 (c) able to mediate transfer of up to 2e⁻ per molecule,²¹ which portends possible application of
 90 ligand-based redox activity in flow batteries for energy storage.²²

91



92

93

Figure 2. C=N containing ligand platforms.

94

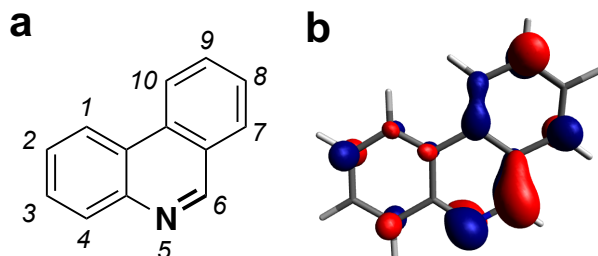
95 At the other extreme, C=N units that comprise delocalized *N*-heterocyclic rings ('pyridine
 96 character') form excellent 'acceptors' for metal-to-ligand charge-transfer (MLCT) electronic
 97 excitations in transition metal coordination complexes. The best studied example²³ is likely the
 98 absorption of visible light by [Ru^{II}(bpy)₃]²⁺ which leads to the formation of a long-lived triplet
 99 excited state through initial MLCT excitation that moves electron density from metal *t*_{2g}-type

100 orbitals into the delocalized π^* manifold of a bpy ligand.¹¹ Given this conceptual continuum of
101 localized to delocalized character, and the prevalence of these systems in exhibiting chemistry
102 from ligand-localized redox to stabilized charge-transfer transitions, we were curious about
103 molecular designs that might enable access to a C=N sub-unit with character intermediate between
104 that of an isolated imine and a more delocalized pyridine.

105 To achieve this, we turned to site-selective benzannulation. Extending benzannulation in
106 pyridine to formulate quinoline (benzo[*b*]pyridine), then the symmetric acridine
107 (dibenzo[*b,e*]pyridine), lowers the energy of the unoccupied orbital manifold, resulting in what
108 should ostensibly be a better acceptor.²⁴ However, if this second benzannulation occurs at the 3,4-
109 position, the asymmetric, tricyclic molecule phenanthridine (benzo[*c*]quinoline) is formed.
110 Compared with quinoline, acridine or the readily cyclometallated benzo[*h*]quinoline (7,8-
111 benzoquinoline)²⁵, phenanthridine (3,4-benzoquinoline) has been much less explored as a ligand
112 in transition metal chemistry. Phenanthridine is not without attractive features: it is respectably
113 fluorescent, which has been exploited in dyes like ethidium bromide and related compounds;²⁶ its
114 planarity has been leveraged in the construction of platinum anti-cancer compounds such as
115 phenanthriplatin (*cis*-[Pt^{II}(NH₃)₂(phenanthridine)Cl]NO₃);²⁷ and it can be reversibly
116 (de)hydrogenated, enabling application as a co-catalyst in hydrogenation reactions.^{28,29} This latter
117 reactivity can be realized electrochemically,³⁰ with implications for *N*-heterocycle-mediated
118 electrochemical CO₂ reduction³¹ and methodologies for electrochemical hydrogenation.³² The
119 ease with which phenanthridine's C=N bond can be selectively reduced can be understood by
120 considering that phenanthridine has three (fused) six-membered rings but only 14 π electrons. The
121 'imine-bridged biphenyl' resonance structure contributes most strongly to the ground state
122 structure as it maximizes the number of aromatic sextets which can be drawn (Figure 3a).³³ This

123 manifests in a solid-state structure with a particularly short C=N bond (1.296(3) Å³⁴) and an
124 unusually downfield chemical shift for the hydrogen nucleus in the C₆ position (9.27 ppm)
125 compared to the *ortho* CH signals in pyridine (8.6 ppm). Benzannulation in this case thus renders
126 the central C₅N ring *less* aromatic (i.e., less ‘pyridine-like’). The lowest unoccupied molecular
127 orbital (LUMO) is accordingly localized at the C=N sub-unit (Figure 3b), lending phenanthridines
128 conceptually similar electron-accepting character as the prototypical redox non-innocent PDI
129 scaffolds discussed above.

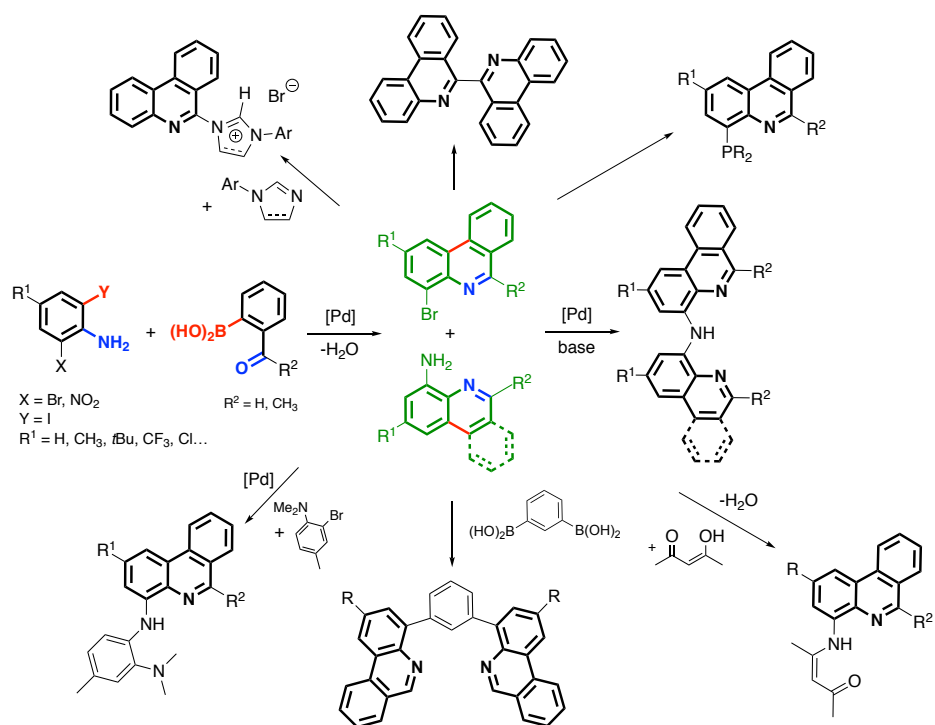
130



131
132 **Figure 3.** (a) Resonance structure of phenanthridine highlighting the ‘imine-like’ character of the
133 C=N sub-unit with the IUPAC numbering scheme given in italics; (b) LUMO of phenanthridine
134 (SMD-M06/Def2-TZVPD//SMD-M06L/Def2-TZVP).

135
136 These observations prompted our investigations into the photophysical properties of
137 phenanthridine-containing coordination complexes. To introduce phenanthridine into the
138 coordination sphere of metals, we targeted bromo- and amino-substituted analogs amenable for
139 elaboration into multidentate scaffolds (Figure 4). We generally access these via a one-pot, tandem
140 Pd-catalyzed cross-coupling/condensation protocol between appropriately substituted anilines and
141 2-formylphenyl boronic acid derivatives.³⁵ From 4-bromo/4-amino phenanthridines, we can then
142 construct P[^]N³⁵, N[^]N^{36,37}, N[^]N[^]N^{38,39}, N[^]N[^]O^{40–42}, N[^]C[^]N⁴³ and N[^]N[^]P⁴⁴ proligands; C[^]N and

143 bpy-style (N^N)₂ biphenanthridine⁴⁵ proligands are available from (6-halo)phenanthridines.⁴⁶
 144 Coordination complexes of these ligands can be used in the Ni-catalyzed direct alkylation of C-H
 145 bonds in azoles,³⁹ as well as to effect acceptorless dehydrogenative coupling reactions in which
 146 alcohols can be employed as electrophiles.⁴⁷ Ru complexes of phenanthridine-containing P^N
 147 ligands can be used in this way to prepare a host of N-heterocycles,⁴⁸ including luminescent⁴⁹ and
 148 donor-acceptor-donor/donor-acceptor-acceptor type pyrimidines.⁵⁰



149
 150 **Figure 4.** Examples of multidentate phenanthridine-containing proligands.

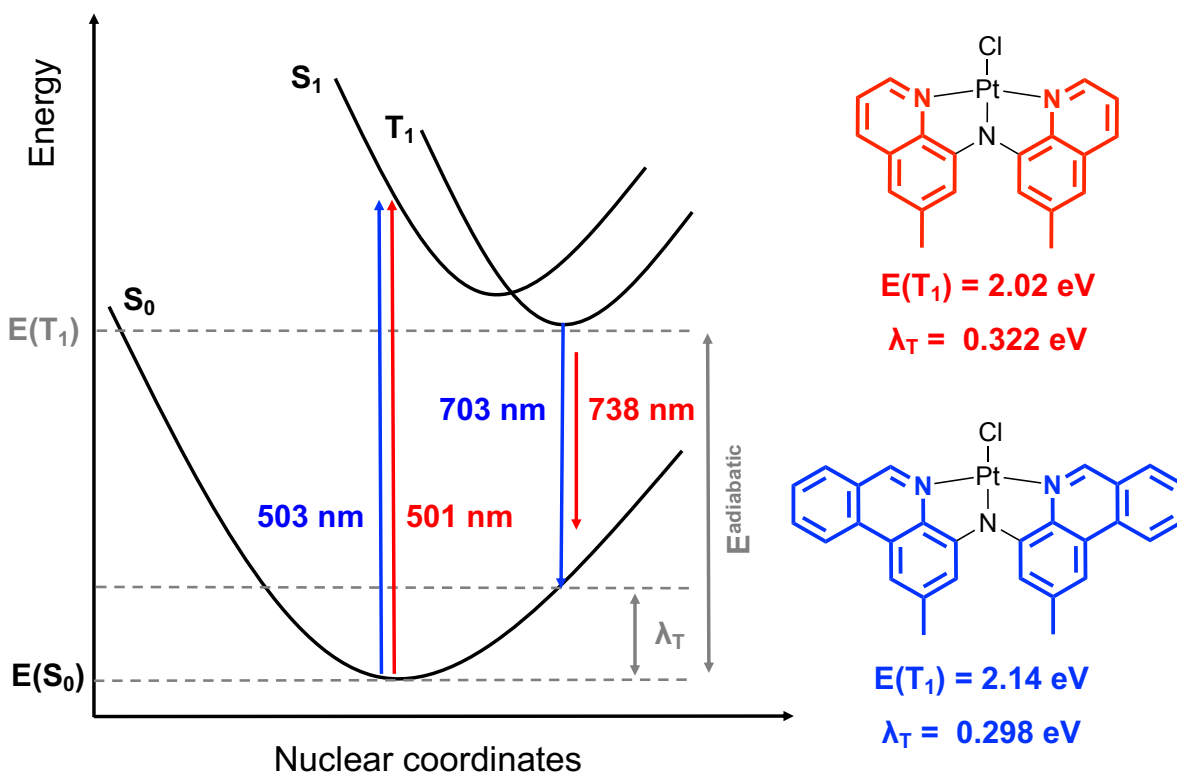
151
 152 Our preparative route to phenanthridine-containing N^N^N ligands followed the
 153 methodology reported by Peters and co-workers for the preparation of *bis*(8-quinolinyl)amido
 154 ‘pincer-type’ ligands.⁵¹ Using Pd-catalyzed coupling of bromo- and amino-substituted 8-
 155 quinolines and 4-phenanthridines, we prepared a series of ligands in which benzannulation is
 156 sequentially expanded from *bis*(8-quinolinyl)amido to (8-quinolinyl)(4-phenanthridinyl)amido to

157 *bis*(4-phenanthridinyl)amido frameworks. These ligands could then be installed on divalent Group
158 10 metal centres to yield a series of complexes that can be thought of as a platform for exploring
159 the impact of systematic, site-selective ligand π -extension.³⁸ Expanding a molecule's π -system is
160 usually associated with a bathochromic shift to its lowest energy absorption and emission
161 processes. This holds true for main-group complexes⁵² as well as transition metal chromophores⁵³
162 and is typically a result of the frontier orbitals growing closer in energy. However, there is a
163 growing literature that describes 'counter-intuitive' hypsochromic blue shifts to both absorption
164 and emission.^{54,55} In one prominent example, Hanson *et al.* demonstrated that (N[^]N[^]N)Pt^{II}Cl
165 complexes of benzannulated *bis*(pyridine)pyrrolate ligands can exhibit either red or blue shifts to
166 absorption and emission maxima.⁵⁶ These observations were rationalized in terms of the site-
167 selective influence of appending a butadiene fragment on the energy of the lowest-unoccupied
168 molecular orbital (LUMO); the highest-occupied molecular orbital (HOMO) was found to be
169 generally unperturbed by benzannulation. This orbital argument was extended to a broader
170 paradigm for small molecules with the caveat that its validity relies on there being a single
171 dominant character to the excitation (absorption) under examination (e.g., HOMO \rightarrow LUMO). This
172 enables application of the Tamm-Dancoff approximation to time-dependent density functional
173 theory (TDDFT)^{57,58} which can be used to validate the orbital analysis.

174 Curiously, our diarylamido-supported Ni(II), Pd(II) and Pt(II) complexes exhibited
175 isoenergetic lowest energy absorption manifolds. For (N[^]N[^]N)Pt^{II}Cl complexes, the character of
176 this excitation was dominantly HOMO \rightarrow LUMO+1.⁵⁹ While the LUMO was found to stabilize
177 with increasing benzannulation in keeping with conventional expectations, the HOMO and
178 LUMO+1 were far less perturbed, leading our complexes to essentially absorb the same energy of
179 visible light irrespective of the presence of quinolinyl or phenanthridinyl side-arms. Interestingly,

180 halide-bridged binuclear Cu(I) complexes of phenanthridinyl-containing P^N ligands did exhibit
181 the ‘expected’ red-shift to the lowest energy absorption manifold compared to quinoline-
182 containing congeners.⁶⁰ However, both Cu(I) and Pt(II) complexes supported by phenanthridinyl
183 ligands phosphoresce at higher energy, with longer excited state lifetimes and higher quantum
184 yields. Contrary to expectations, the quinoline-containing molecules emitted deeper to the red than
185 those exclusively containing phenanthridine heterocycles.

186 In phosphorescent complexes, the (pseudo)Stokes shift is indicative of the degree of
187 geometry reorganization upon excitation and subsequent relaxation to the emissive triplet state.⁶¹
188 Comparing the DFT-optimized ground state (S_0) and lowest-lying triplet states (T_1) for our Pt(II)
189 series, we note that the largest changes to bond lengths in the ligand are localized to the C=N sub-
190 unit for the *bis*(phenanthridinyl)amido complex.⁶² This is not the case in the quinoline-supported
191 complexes, where the distortions in the excited state are more evenly spread about the heterocyclic
192 ligand arms. The imine-localized structure to phenanthridine seems to buffer the rest of the rings
193 from bigger changes upon photoexcitation. So while the formation of triplet states in arenes is
194 generally accompanied by considerable distortion,^{63,64} benzannulation of quinoline to
195 phenanthridine may destabilize the emissive triplet state by inhibiting what would otherwise be an
196 electronically desirable distortion. Overall, phenanthridine-supported Pt(II)^{59,62} and Cu(I) species⁶⁰
197 are more rigid, with smaller differences in the torsion angles estimated for the T_1/S_0 states of the
198 phenanthridine-based systems compared to quinoline-supported analogs - something that can be
199 further exploited through counterion interactions to access even brighter, higher-energy solid-state
200 emitters.⁶⁵ The unexpected blue-shifted emission from phenanthridine-supported Cu(I) and Pt(II)
201 complexes can therefore be ascribed to both a destabilized triplet excited state ($E(T_1)$) and a smaller
202 reorganization energy (λ_T)⁶⁶ upon relaxation back to the ground state (Figure 5).



203
 204 **Figure 5.** Deep-red phosphorescent Pt(II) complexes supported by phenanthridine-containing
 205 ligands. Experimental absorption and emission maxima are reported in nm; DFT-calculated triplet
 206 excited state energies ($E(T_1)$) and reorganization energies (λ_T) are given in eV.

207
 208 Site-selective benzannulation can also help address a curious discrepancy in the literature
 209 noted for emissive Pt(II) complexes of N[^]N[^]N and N[^]C[^]N polypyridyl-type ligands. Namely,
 210 *bis*(quinolinyl)pyridine-supported Pt(II) complexes that form six-membered rings display much
 211 more intense emission than tpy analogs with five-membered rings, an observation attributed to
 212 improved orbital overlap on changing the ligand's bite angle.⁶⁷ However, for cyclometallated N[^]C[^]-
 213 [^]N-coordinated Pt(II) emitters, increasing chelate ring size has the opposite effect: complexes of
 214 6-membered ring forming ligands exhibit much smaller quantum yields ($\Phi_{\text{lum}} = 1.6\%$ for *bis*(8-
 215 quinolinyl)benzene platinum(II) chloride⁶⁷ compared to 60% for *bis*(2-pyridinyl)benzene

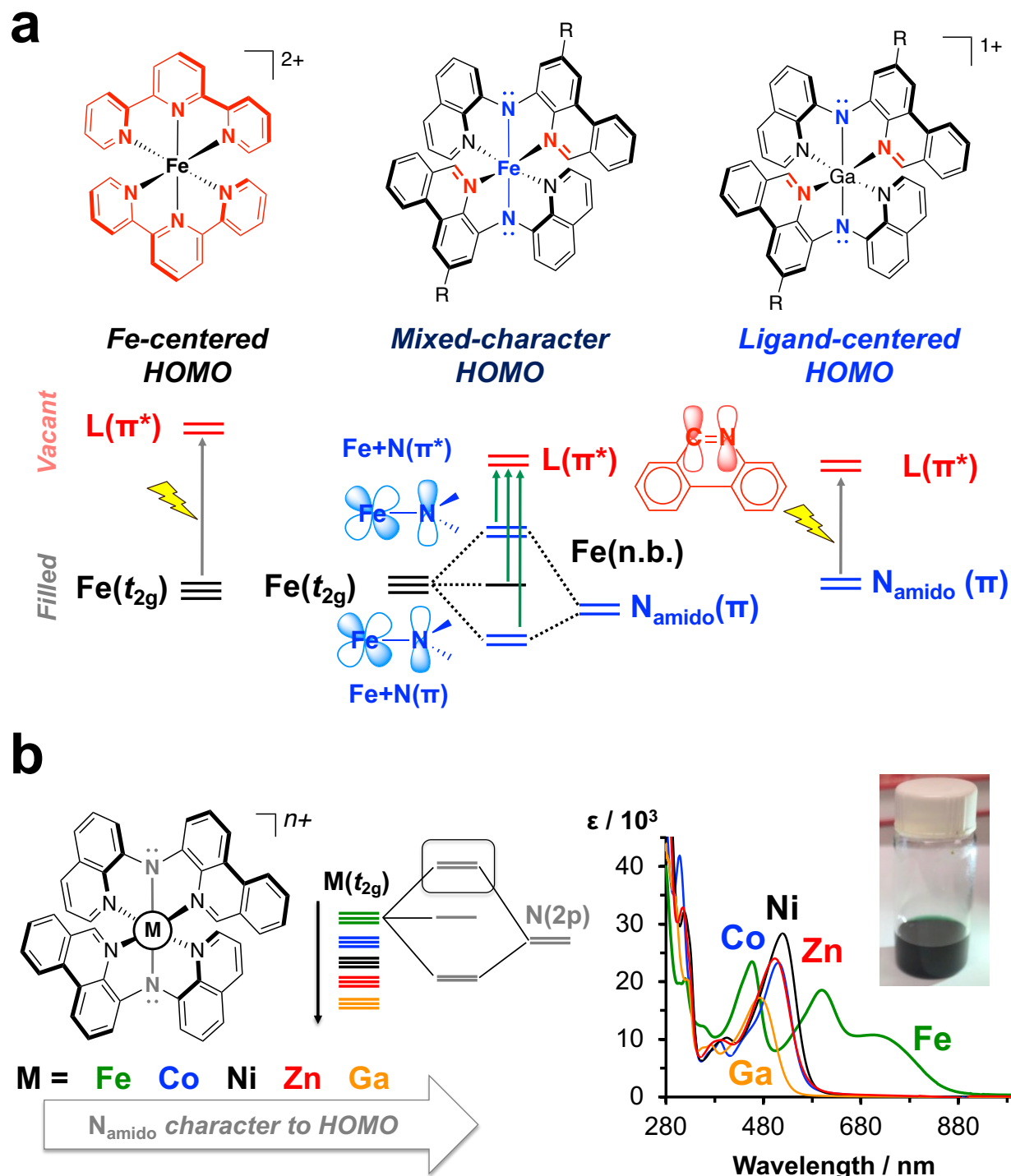
216 platinum(II) chloride⁶⁸). This was traced to significantly lower radiative rate constants attributed
217 to diminished metal participation in the excited state. Site-selective benzannulation of the
218 quinolinyl side-arms to phenanthridine can offset this deleterious effect of changing the chelate
219 ring-size, returning some of the lost emission intensity ($\Phi_{\text{lum}} = 9\%$). Computational analysis
220 suggests benzannulation again destabilizes the emissive triplet state compared to the smaller π -
221 system leading to a smaller (pseudo)Stokes shift, with the localized ‘imine-bridged biphenyl’ form
222 of the phenanthridinyl arms cushioning against larger molecular distortions, improving the
223 quantum yields.⁴³

224 Having established that phenanthridine-containing ligands can present improved ‘acceptor’
225 properties, enhancing molecular rigidity and boosting photophysical properties such as quantum
226 yields and triplet excited state lifetimes, we turned to investigating the impact of these ligand
227 designs on the photoactivity of iron(II) coordination complexes. The question of how to replicate
228 the favourable photophysical properties of precious-metal sensitizers such as $[\text{Ru}^{\text{II}}(\text{bpy})_3]^{2+}$ in
229 complexes of more sustainable elements like iron has received renewed attention of late,⁶⁹ with
230 some of the momentum in this area attributable to seminal experiments on charge-injection from
231 photoexcited Fe(II) complexes into surfaces by Ferrere and Gregg.⁷⁰ The complicating challenge
232 is that in direct analogs of $[\text{Ru}^{\text{II}}(\text{bpy})_3]^{2+}$ such as $[\text{Fe}^{\text{II}}(\text{bpy})_3]^{2+}$, photogenerated ¹MLCT states
233 deactivate on an ultrafast (< 100 fs) timescale down to the ligand field manifold.⁷¹ In most cases,
234 this precludes the possibility for photoinduced electron transfer which typically happens through
235 long-lived charge-transfer states,⁷² although exciting work is emerging that hints at the utility of
236 other mechanisms for excited-state electron transfer.⁷³ A clue as to why can be gleaned from
237 comparing the potential energy curves representing the excited states typical of Ru(II)- and Fe(II)-
238 polypyridyl complexes. Once formed, electron transfer in $[\text{Ru}^{\text{II}}(\text{bpy})_3]^{2+}$ from ^{1/3}MLCT states to

239 metal-centered (MC) states is an activated process, implying that it is slow on the nanosecond or
240 longer time scale. In contrast, for Fe analogs, the crossing between the $^1/3$ MLCT and MC states
241 occurs close to the minimum of the MLCT potential energy curve, which leads to ultrafast decay.⁷⁴
242 This arises from the so-called ‘primogenic effect’⁷⁵ that results in lower overlap and weaker metal-
243 ligand bonds, in turn leading to inversion of excited state character for coordination complexes of
244 the lighter (3d) transition metals compared to their heavier element (4d, 5d) analogs.⁷⁶

245 Efforts to redress this in (pseudo)octahedral Fe(II) complexes have consequently focused
246 on increasing ligand σ -donor strength in an effort to re-order MC/MLCT states by destabilizing
247 metal-centered e_g^* -type orbitals. Pioneering work incorporating increasingly strong σ -donating
248 carbene ligands by the Gros⁷⁷ and Wärnmark^{78,79} groups or cyclometallating C-donor ligands by
249 Dixon,^{80,81} Bauer⁸² and Berkfeld⁸³ have demonstrated the effectiveness of this strategy, enabling
250 high yields of photo-induced charge-injection^{84,85} and the first example of observable room-
251 temperature luminescence from an Fe(II) complex,⁸³ complementing the remarkable discovery of
252 2 LMCT spin-conserved emission from ferric congeners.^{86,87} We were curious about a slightly
253 different approach: what would be the impact of combining strong acceptors like phenanthridine
254 with π -donor amido ligands? Prior to our work, Betley and Peters nicely demonstrated using a
255 simple molecular orbital interaction diagram how orthogonal amido donors might impact the
256 nature of the highest energy manifold in pseudo-octahedral Group VIII complexes,⁸⁸ consistent
257 with the textbook MO treatment of weak-field π -donors.⁸⁹ Indeed, we found installing two
258 equivalents of our phenanthridine-containing diarylamido $N^{\wedge}N^{\wedge}N$ ligands on Fe(II) leads to
259 mixed metal-ligand character of the HOMO through to HOMO-4 thanks to strong mixing between
260 the fully filled, triply degenerate formally t_{2g} orbital set on Fe(II) and the two orthogonal filled
261 N(2p) orbitals (Figure 6a).⁹⁰ This highly covalent character contrasts the situation in $[Fe^{II}(tpy)_2]^{2+}$

262 and Ga(III) complexes of our N[^]N[^]N ligands, and manifests in the Fe-N(amido) distances evident
263 from the solid-state structures of the (N[^]N[^]N)₂Fe(II) and one-electron oxidized [(N[^]N[^]N)₂Fe]⁺.
264 Specifically, removal of an electron from the HOMO depopulates an orbital with Fe-N(amido) π-
265 anti-bonding character and is accompanied by a contraction of the Fe-N(amido) distance from
266 1.932(3)/1.938(3) Å to 1.882(2)/1.901(2) Å for the two crystallographically distinct Fe-N(amido)
267 bonds. The mixed character to the HOMOs also affects the non-zero electric field gradients that
268 can be quantified using zero-field ⁵⁷Fe Mössbauer spectroscopy. Compared with other polypyridyl
269 Fe complexes such as [Fe^{I/III}(tpy)₂]^{2+/3+}, the isomer shifts and quadrupole splitting are not nearly
270 as affected by oxidation for [(N[^]N[^]N)₂Fe]^{0/+}.⁹⁰



271

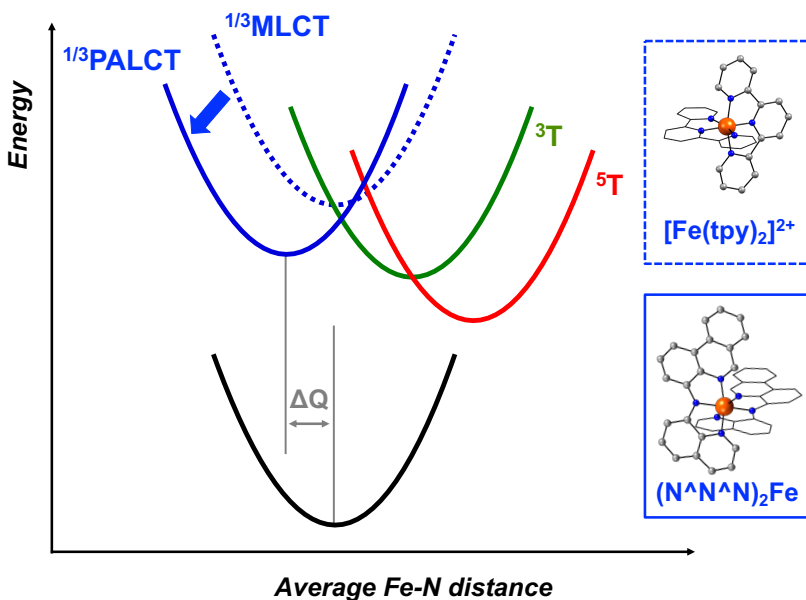
272 **Figure 6.** (a) MO description of strong mixing in iron complexes of weak-field π -donors. (b)

273 Comparing the panchromatic absorption of Fe(II)-amido complexes with increasingly ligand-

274 localized transitions in Co, Ni, Zn and Ga analogs (inset: photograph of a solution of the Fe(II)
275 species).

276

277 These highly covalent Fe-N(amido) interactions lead to strong, panchromatic absorption
278 across the visible range of the electromagnetic spectrum (Figure 6b), in keeping with the
279 predictions of Jakubikova and coworkers about the impact of ‘HOMO inversion’ on the absorption
280 properties of Fe(II) coordination complexes.⁹¹ Altering the energy of the metal orbitals by
281 changing the metal reduces the mixing and yields either metal- (e.g., Ni(II)) or ligand-centered
282 (e.g., for Ga(III)) HOMOs.⁹² Resonant inelastic X-ray scattering experiments confirm this strong
283 covalency and reveal that compared to $[\text{Fe}^{\text{II}}(\text{tpy})_2]^{2+}$, the nephelauxetic reduction in d-electron
284 repulsion thanks to strong Fe-amido mixing counteracts the impact of using weak field π -donor
285 amido ligands on the excited-state ordering at the ground-state geometry.⁹³ Electronic excitation,
286 rather than producing a formally MLCT excited state as for $[\text{Fe}^{\text{II}}(\text{tpy})_2]^{2+}$, forms a “ π -anti-bonding-
287 to-ligand” charge-transfer (PALCT) type excited state (Figure 7).⁹⁴ Transient absorption
288 experiments reveal strong excited-state absorption features that persist for nanoseconds.
289 Assignment of these transiently generated difference spectra using spectroelectrochemistry⁹⁵ is
290 consistent with charge-transfer type character, however without corroborating evidence from the
291 perspective of the metal⁹⁶ this assignment remains incomplete and is the subject of on-going
292 investigations.



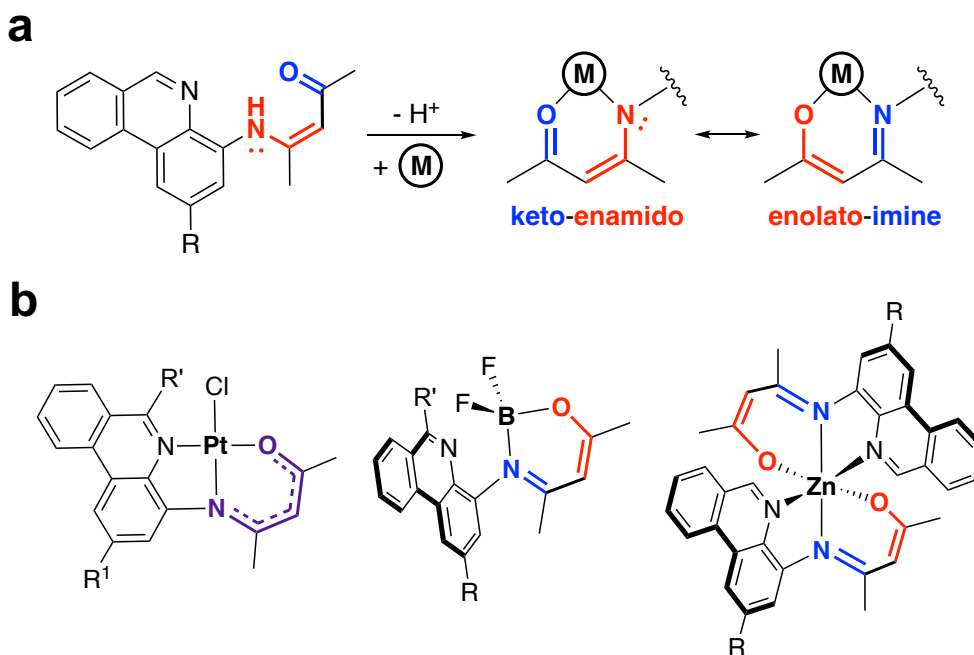
293
 294 **Figure 7.** Schematic potential energy diagram illustrating how increased covalency influences the
 295 nature of the electronic excitation at the ground state geometry ($^{1/3}\text{MLCT}$ for $[\text{Fe}^{\text{II}}(\text{tpy})_2]^{2+}$ vs.
 296 $^{1/3}\text{PALCT}$ excitation in $(\text{N}^{\wedge}\text{N}^{\wedge}\text{N})_2\text{Fe}^{\text{II}}$). The Fe-N bond contraction relative to the ground state
 297 (ΔQ) expected on forming a $^{1/3}\text{PALCT}$ is noted. Also shown are metal-centered triplet (^3T ; green
 298 curve) and quintet (^5T ; red curve) excited states. These high-spin excited states represent the lowest
 299 energy excited states for most pseudo-octahedral polypyridyl Fe(II) coordination complexes,
 300 including $[\text{Fe}^{\text{II}}(\text{tpy})_2]^{2+}$.

301
 302 Consistent with the solid-state structures of the redox-related pair $[(\text{N}^{\wedge}\text{N}^{\wedge}\text{N})_2\text{Fe}]^{0/+}$ noted
 303 above, PALCT should similarly be accompanied by a contraction of the Fe-N(amido) bond
 304 distance (ΔQ), as an anti-bonding orbital is depopulated upon charge-transfer type photoexcitation.
 305 This would contrast the situation on formation of a metal-centered triplet (^3T) or quintet (^5T)
 306 excited state in which metal-ligand σ^* anti-bonding orbitals (i.e., the e_g sub-set) are populated,
 307 causing an elongation of metal-ligand distances.⁹⁷ In principle, stabilizing the CT potential energy

308 surface (PES) and shifting it away from near-lying MC states along the metal-ligand bond
309 coordinate could move the crossing point of the PESs away from the minimum of the PALCT
310 surface. This could suggest a mechanism for introducing an activation barrier that might be used
311 to retard electron transfer from a $^1{}^3$ PALCT excited state to the MC manifold. Indeed, the enhanced
312 covalency of π -donor amido ligands has been used to achieve near-IR-II emission in chromium(III)
313 complexes⁹⁸ and stabilize MLCT excited states with cobalt(III).⁹⁹

314 The amido character of monoanionic pincer-type ligands thus has a significant impact on
315 the photophysical properties of phenanthridine-supported coordination complexes. When
316 tempered by strong mixing with metal-based orbitals as in the Fe(II) example discussed above, or
317 in divalent Group 10 compounds,^{38,39} the presence of the formal nitrogen lone pair does not
318 dominate the chemical reactivity of the complexes and these species are for the most part stable to
319 air and ambient moisture. However, when ligated, for example, to Zn(II), this mixing is limited
320 and Zn(II) complexes of bidentate *N*-aryl phenanthridinyl amides³⁶ or tridentate diarylamido
321 ligands⁹² are quite reactive towards protonolysis by even trace moisture. In contrast, $N^{\wedge}N^{\wedge}O$
322 proligands comprised of ‘nac-ac’ style scaffolds can similarly be used to tone down the lone-pair
323 character of amido ligands, but through contribution of an enolato-imine resonance structure
324 (Figure 8a). Pt(II) complexes of such ligands are much more brightly emissive than
325 phenanthridine-supported ($N^{\wedge}N^{\wedge}N$)Pt(II) chlorides, with phosphorescence quantum yields
326 reaching 16% and 24 microsecond lifetimes.⁴¹ These complexes are also substantially
327 solvatochromic, with a strong influence of the solvent dielectric on the energy of the lowest energy
328 absorption consistent with charge-transfer character.

329



330

331 **Figure 8.** (a) ‘Nac-ac’ style N^NO prolignands and their resonance structures upon metalation; (b)

332 Platinum(II), zinc(II) and boron complexes of N^NO ligands.

333

334 Phenanthridinyl-decorated, β-ketoiminate chelating ligand scaffolds can also be used to

335 construct boron difluoride complexes (Figure 8b).⁴² Here, the BF₂ fragment is four-coordinate,

336 ligated within the ketoiminate N^NO pocket. ¹⁹F–¹H NOE NMR spectroscopy measurements show

337 well-resolved through-space interactions between a phenanthridinyl C–H and one fluorine

338 indicating that in fluid solution the relative orientation of the pendent phenanthridinyl arm is still

339 fixed despite not coordinating to boron. Nevertheless, with nonradiative decay pathways available

340 thanks to rotation of the N-heterocycle, these compounds are only weakly luminescent; however,

341 methylation of the phenanthridinyl nitrogen can be used to ‘switch on’ relatively strong emission

342 by limiting this rotation and altering the character of the lowest energy excitation. Pseudo-

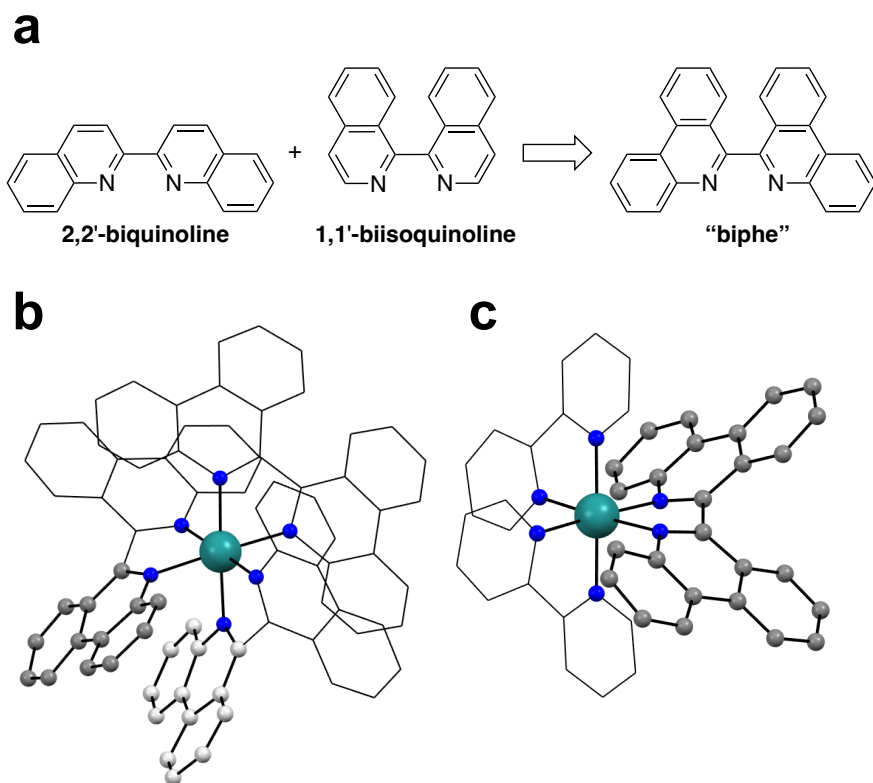
343 octahedral Zn(II) complexes supported by such monoanionic, tridentate acetylacetonone-derived

344 N^NO ligands also emit weakly in solution but exhibit very long (millisecond) luminescence

345 lifetimes when rigidified in the solid state at room temperature or in a frozen glass at 77 K,
346 consistent with phosphorescence from low-lying triplet excited states which is rare for Zn.¹⁰⁰ This
347 is in sharp contrast to non-emissive, four-coordinate, amide-supported tetradentate Zn(II)
348 complexes.³⁶ In addition, the six-coordinate Zn complexes are air- and moisture-stable, as well as
349 unreactive towards mildly acidic solvents. The delocalized character of the central deprotonated
350 NH upon coordination mitigates the amido character of the ligand, increasing chemical stability
351 and provides a mechanism for switching on remarkably long-lived luminescence from *N*-
352 heterocycle/amido-supported Zn(II) coordination complexes.

353 Finally, phenanthridines can be used to prepare doubly π -extended analogs of the canonical
354 ligand 2,2-bipyridyl (bpy) we termed “biphe” (6,6'-biphenanthridine; Figure 9a).⁴⁵ The organic
355 proligand itself displays blue fluorescence in solution, which shifts to even stronger yellow
356 emission upon monoprotection. *Tris*(6,6'-biphenanthridine)ruthenium(II) and *bis*(2,2'-
357 bipyridine)(6,6'-biphenanthridine)ruthenium(II) dications can also be made and these display
358 strongly bathochromically shifted emission at 77 K that is nearly 200 nm red-shifted compared to
359 $[\text{Ru}^{\text{II}}(\text{bpy})_3]^{2+}$. This phosphorescence is very weak and short-lived at ambient temperature,
360 however, and rapid ligand photodissociation competes with radiative decay, especially in the
361 heteroleptic complex. Nevertheless, this substantial low energy shift is consistent with the lower
362 energy π^* orbitals that accompany extended conjugation, which lowers the energy of the emissive
363 $^3\text{MLCT}$ excited state. Indeed, biphe's stabilized vacant π^* manifold can be addressed
364 electrochemically, and multiple reversible reductions are observed by cyclic voltammetry at much
365 less negative potentials compared with $[\text{Ru}^{\text{II}}(\text{bpy})_3]^{2+}$. As can be seen from the solid-state
366 structures in Figure 9b, the biphe ligand is significantly twisted despite chelating to the metal and

367 our current efforts are addressing this lack of planarity in order to boost the efficiency of any low-
368 energy emission.



369
370 **Figure 9.** (a) π -extended bpy analogs and solid-state structures of (b) *tris*(6,6'-
371 biphenanthridine)ruthenium(II) dication showing intramolecular π -stacking between biphe
372 ligands and (c) *bis*(2,2'-bipyridine)(6,6'-biphenanthridine)ruthenium(II) dication illustrating the
373 twist between phenanthridine units in coordinated biphe.

374

375

376 **Conclusion and Outlook**

377 Large, planar *N*-heterocyclic frameworks provide a rich playground for coordination chemistry,¹⁰¹
378 one that is continually revealing interesting nuances with respect to the impact of site-selective
379 benzannulation on commonly held conceptions regarding ligand π -extension. In particular, *N*-
380 heterocycles, that through the quirks of their structures present ‘imine-like’ C=N units, can help
381 rigidify molecular scaffolds, attenuating non-radiative decay and increasing both excited state
382 lifetimes and quantum yields. When paired with weak-field amido donors, highly covalent
383 molecules can be designed and constructed that strongly absorb wide swathes of visible light with
384 unexpected excited-state properties. The findings surveyed in this article suggest that simple
385 structural changes may continue to lead to the discovery of novel ligand and molecular designs
386 with yet unanticipated fascinating fundamental properties and the possibility of useful
387 applications.

388

389

390 **AUTHOR INFORMATION**

391 **Corresponding Author**

392 David E. Herbert (david.herbert@umanitoba.ca)

393 **ORCIDs**

394 David E. Herbert: 0000-0001-8190-2468

395

396 **ACKNOWLEDGMENTS**

397 I am grateful to the Canadian Society for Chemistry and Strem Chemicals for the 2022 *Strem*
398 *Chemicals Award for Pure or Applied Chemistry*. This award is a testament to the talents and
399 efforts of the many undergraduates, graduate students, and postdoctoral fellows I have been
400 fortunate to work with at the University of Manitoba (UM), and extraordinary collaborators both
401 at UM and elsewhere whose names appear in the references included in this article. The ideas
402 presented here were, without exception, developed through stimulating, close cooperation; it has
403 been a privilege to conduct and discuss science with them all. I also thank the Natural Sciences
404 Engineering Research Council of Canada, the Canada Foundation for Innovation, Research
405 Manitoba, and the University of Manitoba for supporting discovery-based science in Manitoba and
406 Canada in general, and within my research and training program in particular. Finally, Issiah B.
407 Lozada is thanked for the calculated isosurface which appears in Figure 3b.

408

409 **Competing Interests Statement**

410 The author declares no competing interests.

411 **Data Availability Statement**

412 This manuscript is a review article and does not report new data.

413 REFERENCES

- 414 (1) Fryzuk, M. D. The 1992 Alcan Award Lecture Excursions around the Periodic Table:
415 Ligand Design in Inorganic Chemistry. *Can. J. Chem.* **1992**, *70*, 2839–2845.
- 416 (2) Chirik, P. J.; Wieghardt, K. Radical Ligands Confer Nobility on Base-Metal Catalysts.
417 *Science* **2010**, *327*, 794–795.
- 418 (3) Bullock, R. M. Abundant Metals Give Precious Hydrogenation Performance. *Science*
419 **2013**, *342*, 1054–1055.
- 420 (4) Chirik, P. J. Iron- and Cobalt-Catalyzed Alkene Hydrogenation: Catalysis with Both
421 Redox-Active and Strong Field Ligands. *Acc. Chem. Res.* **2015**, *48*, 1687–1695.
- 422 (5) Dierks, P.; Vukadinovic, Y.; Bauer, M. Photoactive Iron Complexes: More Sustainable,
423 but Still a Challenge. *Inorg. Chem. Front.* **2022**, *9*, 206–220.
- 424 (6) Zhang, C.; Zhang, L.; Ding, Y.; Peng, S.; Guo, X.; Zhao, Y.; He, G.; Yu, G. Progress and
425 Prospects of Next-Generation Redox Flow Batteries. *Energ. Stor. Mater.* **2018**, *15*, 324–
426 350.
- 427 (7) Evans, B. E.; Rittle, K. E.; Bock, M. G.; DiPardo, R. M.; Freidinger, R. M.; Whitter, W.
428 L.; Lundell, G. F.; Veber, D. F.; Anderson, P. S.; Chang, R. S. L.; Lotti, V. J.; Cerino, D.
429 J.; Chen, T. B.; Kling, P. J.; Kunkel, K. A.; Springer, J. P.; Hirshfield, J. Methods for Drug
430 Discovery: Development of Potent, Selective, Orally Effective Cholecystokinin
431 Antagonists. *J. Med. Chem.* **1988**, *31*, 2235–2246.
- 432 (8) Yoon, T. P.; Jacobsen, E. N. Privileged Chiral Catalysts. *Science* **2003**, *299*, 1691–1693.
- 433 (9) Lyaskovskyy, V.; de Bruin, B. Redox Non-Innocent Ligands: Versatile New Tools to
434 Control Catalytic Reactions. *ACS Catal.* **2012**, *2*, 270–279.
- 435 (10) Gunanathan, C.; Milstein, D. Metal-Ligand Cooperation by Aromatization-
436 Dearomatization: A New Paradigm in Bond Activation and “Green” Catalysis. *Acc. Chem.*
437 *Res.* **2011**, *44*, 588–602.
- 438 (11) Juris, A.; Balzani, V.; Barigelletti, F.; Campagna, S.; Belser, P.; Von Zelewsky, A.
439 Ruthenium(II) Polypyridine Complexes: Photophysics, Photochemistry, Electrochemistry,
440 and Chemiluminescence. *Coord. Chem. Rev.* **1988**, *84*, 85–277.
- 441 (12) Koten, G. V.; Vrieze, K. 1,4-Diaza-1,3-Butadiene (α -Diimine) Ligands: Their
442 Coordination Modes and the Reactivity of Their Metal Complexes. *Adv. Organomet.*
443 *Chem.* **1982**, *21*, 151–239.
- 444 (13) Flisak, Z.; Sun, W.-H. Progression of Diiminopyridines: From Single Application to
445 Catalytic Versatility. *ACS Catal.* **2015**, *5*, 4713–4724.
- 446 (14) Thummel, R. P. Terpyridine, Oligopyridine, and Polypyridine Ligands. In *Compr. Coord.*
447 *Chem. II*; Elsevier Ltd., 2004; Vol. 1, pp 41–53.
- 448 (15) Singh, K.; Kundu, A.; Adhikari, D. Ligand-Based Redox: Catalytic Applications and
449 Mechanistic Aspects. *ACS Catal.* **2022**, *12*, 13075–13107.
- 450 (16) Gray, P. A.; Braun, J. D.; Rahimi, N.; Herbert, D. E. Diiminepyridine-Supported
451 Phosphorus(I) and Phosphorus(III) Complexes: Synthesis, Characterization, and
452 Electrochemistry. *Eur. J. Inorg. Chem.* **2020**, *2020*, 2105–2111.
- 453 (17) Tondreau, A. M.; Stieber, S. C. E.; Milsman, C.; Lobkovsky, E.; Weyhermuller, T.;
454 Semproni, S. P.; Chirik, P. J. Oxidation and Reduction of Bis(Imino)Pyridine Iron
455 Dinitrogen Complexes: Evidence for Formation of a Chelate Trianion. *Inorg. Chem.* **2013**,
456 *52*, 635–646.

- 457 (18) Kiernicki, J. J.; Fanwick, P. E.; Bart, S. C. Utility of a Redox-Active Pyridine(Diimine)
458 Chelate in Facilitating Two Electron Oxidative Addition Chemistry at Uranium. *Chem.*
459 *Commun.* **2014**, *50*, 8189–8192.
- 460 (19) de Bruin, B.; Bill, E.; Bothe, E.; Weyhermueller, T.; Wieghardt, K. Molecular and
461 Electronic Structures of Bis(Pyridine-2,6-Diimine)Metal Complexes [ML₂](PF₆)_n (n = 0,
462 1, 2, 3; M = Mn, Fe, Co, Ni, Cu, Zn). *Inorg. Chem.* **2000**, *39*, 2936–2947.
- 463 (20) Duarte, G. M.; Braun, J. D.; Giesbrecht, P. K.; Herbert, D. E. Redox Non-Innocent
464 Bis(2,6-Diimine-Pyridine) Ligand-Iron Complexes as Anolytes for Flow Battery
465 Applications. *Dalton Trans.* **2017**, *46*, 16439–16445.
- 466 (21) Braun, J. D.; Gray, P. A.; Sidhu, B. K.; Nemez, D. B.; Herbert, D. E. Zn-Templated
467 Synthesis of Substituted (2,6-Diimine)Pyridine Proligands and Evaluation of Their Iron
468 Complexes as Anolytes for Flow Battery Applications. *Dalton Trans.* **2020**, *49*, 16175–
469 16183.
- 470 (22) Soloveichik, G. L. Flow Batteries: Current Status and Trends. *Chem. Rev.* **2015**, *115*,
471 11533–11558.
- 472 (23) Arias-Rotondo, D. M. The Fruit Fly of Photophysics. *Nat. Chem.* **2022**, *14*, 716–716.
- 473 (24) Katritzky, A. R. *Handbook of Heterocyclic Chemistry*, 3rd ed.; Oxford : Elsevier: Oxford,
474 2010.
- 475 (25) Neufeldt, S. R.; Sanford, M. S. Controlling Site Selectivity in Palladium-Catalyzed C–H
476 Bond Functionalization. *Acc. Chem. Res.* **2012**, *45*, 936–946.
- 477 (26) Tumir, L.-M.; Stojkovic, M. R.; Piantanida, I. Come-Back of Phenanthridine and
478 Phenanthridinium Derivatives in the 21st Century. *Beilstein J. Org. Chem.* **2014**, *10*,
479 2930–2954.
- 480 (27) Johnstone, T. C.; Park, G. Y.; Lippard, S. J. Understanding and Improving Platinum
481 Anticancer Drugs - Phenanthriplatin. *Anticancer Res.* **2014**, *34*, 471–476.
- 482 (28) Chen, Q.-A.; Gao, K.; Duan, Y.; Ye, Z.-S.; Shi, L.; Yang, Y.; Zhou, Y.-G.
483 Dihydrophenanthridine: A New and Easily Regenerable NAD(P)H Model for Biomimetic
484 Asymmetric Hydrogenation. *J. Am. Chem. Soc.* **2012**, *134*, 2442–2448.
- 485 (29) Lu, L.-Q.; Li, Y.; Junge, K.; Beller, M. Iron-Catalyzed Hydrogenation for the In Situ
486 Regeneration of an NAD(P)H Model: Biomimetic Reduction of α -Keto-/ α -Iminoesters.
487 *Angew. Chem., Int. Ed.* **2013**, *52*, 8382–8386.
- 488 (30) Giesbrecht, P. K.; Nemez, D. B.; Herbert, D. E. Electrochemical Hydrogenation of a
489 Benzannulated Pyridine to a Dihydropyridine in Acidic Solution. *Chem. Commun.* **2018**,
490 *54*, 338–341.
- 491 (31) Giesbrecht, P. K.; Herbert, D. E. Electrochemical Reduction of Carbon Dioxide to
492 Methanol in the Presence of Benzannulated Dihydropyridine Additives. *ACS Energy Lett.*
493 **2017**, *2*, 549–555.
- 494 (32) Nemez, D. B.; Sidhu, B. K.; Giesbrecht, P. K.; Braun, J. D.; Herbert, D. E.
495 Electrochemical Hydrogenation of α -Ketoesters and Benzoxazinones Using Carbon
496 Electrodes and a Sustainable Brønsted Acid. *Org. Chem. Front.* **2021**, *8*, 549–554.
- 497 (33) Maksic, Z. B.; Baric, D.; Mueller, T. Clar's Sextet Rule Is a Consequence of the σ -
498 Electron Framework. *J. Phys. Chem. A* **2006**, *110*, 10135–10147.
- 499 (34) Brett, W. A.; Rademacher, P.; Boese, R. Redetermination of the Structure of
500 Phenanthridine. *Acta Crystallogr., Sect. C: Cryst. Struct. Commun.* **1993**, *C49*, 1564–
501 1566.

- 502 (35) Mondal, R.; Giesbrecht, P. K.; Herbert, D. E. Nickel(II), Copper(I) and Zinc(II)
503 Complexes Supported by a (4-Diphenylphosphino)Phenanthridine Ligand. *Polyhedron*
504 **2016**, *108*, 156–162.
- 505 (36) Lozada, I. B.; Murray, T.; Herbert, D. E. Monomeric Zinc(II) Amide Complexes
506 Supported by Bidentate, Benzannulated Phenanthridine Amido Ligands. *Polyhedron* **2019**,
507 *161*, 261–267.
- 508 (37) Gaire, S.; Ortiz, R. J.; Schrage, B. R.; Lozada, I. B.; Mandapati, P.; Osinski, A. J.; Herbert,
509 D. E.; Ziegler, C. J. (8-Amino)Quinoline and (4-Amino)Phenanthridine Complexes of
510 $\text{Re}(\text{CO})_3$ Halides. *J. Organomet. Chem.* **2020**, *921*, 121338.
- 511 (38) Mandapati, P.; Giesbrecht, P. K.; Davis, R. L.; Herbert, D. E. Phenanthridine-Containing
512 Pincer-like Amido Complexes of Nickel, Palladium, and Platinum. *Inorg. Chem.* **2017**, *56*,
513 3674–3685.
- 514 (39) Mandapati, P.; Braun, J. D.; Sidhu, B. K.; Wilson, G.; Herbert, D. E. Catalytic C–H Bond
515 Alkylation of Azoles with Alkyl Halides Mediated by Nickel(II) Complexes of
516 Phenanthridine-Based $\text{N}^{\wedge}\text{N}^{\wedge}\text{N}$ Pincer Ligands. *Organometallics* **2020**, *39*, 1989–1997.
- 517 (40) Lozada, I. B.; Huang, B.; Stilgenbauer, M.; Beach, T.; Qiu, Z.; Zheng, Y.; Herbert, D. E.
518 Monofunctional Platinum(II) Anticancer Complexes Based on Multidentate
519 Phenanthridine-Containing Ligand Frameworks. *Dalton Trans.* **2020**, *49*, 6557–6560.
- 520 (41) Lozada, I. B.; Williams, J. A. G.; Herbert, D. E. Platinum(II) Complexes of Benzannulated
521 $\text{N}^{\wedge}\text{N}^{\wedge}\text{O}$ -Amido Ligands: Bright Orange Phosphors with Long-Lived Excited States.
522 *Inorg. Chem. Front.* **2022**, *9*, 10–22.
- 523 (42) Lozada, I. B.; Ortiz, R. J.; Braun, J. D.; Williams, J. A. G.; Herbert, D. E. Donor–Acceptor
524 Boron-Ketoiminate Complexes with Pendent *N*-Heterocyclic Arms: Switched-on
525 Luminescence through *N*-Heterocycle Methylation. *J. Org. Chem.* **2022**, *87*, 184–196.
- 526 (43) Ortiz, R. J.; Braun, J. D.; Williams, J. A. G.; Herbert, D. E. Brightly Luminescent
527 Platinum Complexes of $\text{N}^{\wedge}\text{C}^{\wedge}\text{N}$ Ligands Forming Six-Membered Chelate Rings:
528 Offsetting Deleterious Ring Size Effects Using Site-Selective Benzannulation. *Inorg.*
529 *Chem.* **2021**, *60*, 16881–16894.
- 530 (44) Sidhu, B. K.; Braun, J. D.; Herbert, D. E. P–C Bond Activation and Transfer of a
531 Diphenylphosphino Unit from 1,1'-Bis(Diphenylphosphino)Ferrocene: Unexpected
532 Templated Synthesis of an $\text{N}^{\wedge}\text{N}^{\wedge}\text{P}$ Pincer Ligand Palladium Complex. *Organometallics*
533 **2021**, *40*, 2538–2545.
- 534 (45) Nemez, D. B.; Lozada, I. B.; Braun, J. D.; Williams, J. A. G.; Herbert, D. E. Synthesis and
535 Coordination Chemistry of a Benzannulated Bipyridine: 6,6'-Biphenanthridine. *Inorg.*
536 *Chem.* **2022**, *61*, 13386–13398.
- 537 (46) Mondal, R.; Ortiz, R. J.; Braun, J. D.; Herbert, D. E. Synthesis, Characterization, and
538 Coordination Chemistry of a Phenanthridine-Containing *N*-Heterocyclic Carbene Ligand.
539 *Can. J. Chem.* **2021**, *99*, 245–252.
- 540 (47) Gunanathan, C.; Milstein, D. Applications of Acceptorless Dehydrogenation and Related
541 Transformations in Chemical Synthesis. *Science* **2013**, *341*, 249.
- 542 (48) Mondal, R.; Herbert, D. E. Synthesis of Pyridines, Quinolines, and Pyrimidines via
543 Acceptorless Dehydrogenative Coupling Catalyzed by a Simple Bidentate $\text{P}^{\wedge}\text{N}$ Ligand
544 Supported Ru Complex. *Organometallics* **2020**, *39*, 1310–1317.
- 545 (49) Mondal, R.; Lozada, I. B.; Stotska, O.; Herbert, D. E. Catalytic Synthesis of Luminescent
546 Pyrimidines via Acceptor-Less Dehydrogenative Coupling. *J. Org. Chem.* **2020**, *85*,
547 13747–13756.

- 548 (50) Mondal, R.; Braun, J. D.; Sidhu, B. K.; Nevenon, D. E.; Nemykin, V. N.; Herbert, D. E.
549 Catalytic Synthesis of Donor-Acceptor-Donor (D-A-D) and Donor-Acceptor-Acceptor (D-
550 A-A) Pyrimidine-Ferrocenes via Acceptorless Dehydrogenative Coupling: Synthesis,
551 Structures, and Electronic Communication. *Organometallics* **2021**, *40*, 1765–1775.
- 552 (51) Peters, J. C.; Harkins, S. B.; Brown, S. D.; Day, M. W. Pincer-like Amido Complexes of
553 Platinum, Palladium, and Nickel. *Inorg. Chem.* **2001**, *40*, 5083–5091.
- 554 (52) Barbon, S. M.; Staroverov, V. N.; Gilroy, J. B. Effect of Extended π Conjugation on the
555 Spectroscopic and Electrochemical Properties of Boron Difluoride Formazanate
556 Complexes. *J. Org. Chem.* **2015**, *80*, 5226–5235.
- 557 (53) Li, Z.; Cui, P.; Wang, C.; Kilina, S.; Sun, W. Nonlinear Absorbing Cationic Bipyridyl
558 Iridium(III) Complexes Bearing Cyclometalating Ligands with Different Degrees of π -
559 Conjugation: Synthesis, Photophysics, and Reverse Saturable Absorption. *J. Phys. Chem.*
560 *C* **2014**, *118*, 28764–28775.
- 561 (54) Bossi, A.; Rausch, A. F.; Leitzl, M. J.; Czerwieniec, R.; Whited, M. T.; Djurovich, P. I.;
562 Yersin, H.; Thompson, M. E. Photophysical Properties of Cyclometalated Pt(II)
563 Complexes: Counterintuitive Blue Shift in Emission with an Expanded Ligand π System.
564 *Inorg. Chem.* **2013**, *52*, 12403–12415.
- 565 (55) Liu, B.; Lystrom, L.; Brown, S. L.; Hobbie, E. K.; Kilina, S.; Sun, W. Impact of
566 Benzannulation Site at the Diimine ($N^{\wedge}N$) Ligand on the Excited-State Properties and
567 Reverse Saturable Absorption of Biscyclometalated Iridium(III) Complexes. *Inorg. Chem.*
568 **2019**, *58*, 5483–5493.
- 569 (56) Hanson, K.; Roskop, L.; Djurovich, P. I.; Zahariev, F.; Gordon, M. S.; Thompson, M. E. A
570 Paradigm for Blue- or Red-Shifted Absorption of Small Molecules Depending on the Site
571 of π -Extension. *J. Am. Chem. Soc.* **2010**, *132*, 16247–16255.
- 572 (57) Hirata, S.; Head-Gordon, M. Time-Dependent Density Functional Theory within the
573 Tamm–Dancoff Approximation. *Chem. Phys. Lett.* **1999**, *314*, 291–299.
- 574 (58) Dreuw, A.; Head-Gordon, M. Single-Reference Ab Initio Methods for the Calculation of
575 Excited States of Large Molecules. *Chem. Rev.* **2005**, *105*, 4009–4037.
- 576 (59) Mandapati, P.; Braun, J. D.; Killeen, C.; Davis, R. L.; Williams, J. A. G.; Herbert, D. E.
577 Luminescent Platinum(II) Complexes of $N^{\wedge}N^{\wedge}N$ Amido Ligands with Benzannulated N -
578 Heterocyclic Donor Arms: Quinolines Offer Unexpectedly Deeper Red Phosphorescence
579 than Phenanthridines. *Inorg. Chem.* **2019**, *58*, 14808–14817.
- 580 (60) Mondal, R.; Lozada, I. B.; Davis, R. L.; Williams, J. A. G.; Herbert, D. E. Site-Selective
581 Benzannulation of N -Heterocycles in Bidentate Ligands Leads to Blue-Shifted Emission
582 from $[(P^{\wedge}N)Cu]_2(\mu-X)_2$ Dimers. *Inorg. Chem.* **2018**, *57*, 4966–4978.
- 583 (61) Shon, J.-H.; Teets, T. S. Molecular Photosensitizers in Energy Research and Catalysis:
584 Design Principles and Recent Developments. *ACS Energy Lett.* **2019**, *4*, 558–566.
- 585 (62) Mandapati, P.; Braun, J. D.; Lozada, I. B.; Williams, J. A. G.; Herbert, D. E. Deep-Red
586 Luminescence from Platinum(II) Complexes of $N^{\wedge}N^{\wedge}N$ -Amido Ligands with
587 Benzannulated N -Heterocyclic Donor Arms. *Inorg. Chem.* **2020**, *59*, 12504–12517.
- 588 (63) de Groot, M. S.; van der Waals, J. H. Paramagnetic Resonance in Phosphorescent
589 Aromatic Hydrocarbons. III. Conformational Isomerism in Benzene and Triptycene. *Mol.*
590 *Phys.* **1963**, *6*, 545.
- 591 (64) Papadakis, R.; Ottosson, H. The Excited State Antiaromatic Benzene Ring: A Molecular
592 Mr Hyde? *Chem. Soc. Rev.* **2015**, *44*, 6472–6493.

- 593 (65) Mondal, R.; Lozada, I. B.; Davis, R. L.; Williams, J. A. G.; Herbert, D. E. Exploiting
594 Synergy between Ligand Design and Counterion Interactions to Boost Room Temperature
595 Phosphorescence from Cu(I) Compounds. *J. Mater. Chem. C* **2019**, *7*, 3772–3778.
- 596 (66) Uoyama, H.; Goushi, K.; Shizu, K.; Nomura, H.; Adachi, C. Highly Efficient Organic
597 Light-Emitting Diodes From Delayed Fluorescence. *Nature* **2012**, *492*, 234–238.
- 598 (67) Garner, K. L.; Parkes, L. F.; Piper, J. D.; Williams, J. A. G. Luminescent Platinum
599 Complexes with Tridentate Ligands Forming 6-Membered Chelate Rings: Advantageous
600 and Deleterious Effects in N^NN and N^CN-Coordinated Complexes. *Inorg. Chem.*
601 **2010**, *49*, 476–487.
- 602 (68) Williams, J. A. G. The Coordination Chemistry of Dipyridylbenzene: N-Deficient
603 Terpyridine or Panacea for Brightly Luminescent Metal Complexes? *Chem. Soc. Rev.*
604 **2009**, *38*, 1783–1801.
- 605 (69) Wenger, O. S. Is Iron the New Ruthenium? *Chem. - Eur. J.* **2019**, *25*, 6043–6052.
- 606 (70) Ferrere, S.; Gregg, B. A. Photosensitization of TiO₂ by [Fe^{II}(2,2'-Bipyridine-4,4'-
607 Dicarboxylic Acid)₂(CN)₂]: Band Selective Electron Injection from Ultra-Short-Lived
608 Excited States. *J. Am. Chem. Soc.* **1998**, *120*, 843–844.
- 609 (71) Juban, E. A.; Smeigh, A. L.; Monat, J. E.; McCusker, J. K. Ultrafast Dynamics of Ligand-
610 Field Excited States. *Coord. Chem. Rev.* **2006**, *250*, 1783–1791.
- 611 (72) Arias-Rotondo, D. M.; McCusker, J. K. The Photophysics of Photoredox Catalysis: A
612 Roadmap for Catalyst Design. *Chem. Soc. Rev.* **2016**, *45*, 5803–5820.
- 613 (73) Woodhouse, M. D.; McCusker, J. K. Mechanistic Origin of Photoredox Catalysis
614 Involving Iron(II) Polypyridyl Chromophores. *J. Am. Chem. Soc.* **2020**, *142* (38), 16229–
615 16233.
- 616 (74) Ponseca, C. S.; Chabera, P.; Uhlig, J.; Persson, P.; Sundstroem, Villy. Ultrafast Electron
617 Dynamics in Solar Energy Conversion. *Chem. Rev.* **2017**, *117*, 10940–11024.
- 618 (75) Kaupp, M. The Role of Radial Nodes of Atomic Orbitals for Chemical Bonding and the
619 Periodic Table. *J. Comput. Chem.* **2007**, *28*, 320–325.
- 620 (76) McCusker, J. K. Electronic Structure in the Transition Metal Block and Its Implications
621 for Light Harvesting. *Science* **2019**, *363*, 484.
- 622 (77) Duchanois, T.; Liu, L.; Pastore, M.; Monari, A.; Cebrián, C.; Trolez, Y.; Darari, M.;
623 Magra, K.; Francés-Monerris, A.; Domenichini, E.; Beley, M.; Assfeld, X.; Haacke, S.;
624 Gros, P. C. NHC-Based Iron Sensitizers for DSSCs. *Inorganics* **2018**, *6*, 63.
- 625 (78) Liu, Y.; Warnmark, K.; Liu, Y.; Sundstrom, V.; Persson, P. Fe N-Heterocyclic Carbene
626 Complexes as Promising Photosensitizers. *Acc. Chem. Res.* **2016**, *49*, 1477–1485.
- 627 (79) Chábera, P.; Kjaer, K. S.; Prakash, O.; Honarfar, A.; Liu, Y.; Fredin, L. A.; Harlang, T. C.
628 B.; Lidin, S.; Uhlig, J.; Sundström, V.; Lomoth, R.; Persson, P.; Wärnmark, K. FeII Hexa
629 N-Heterocyclic Carbene Complex with a 528 Ps Metal-to-Ligand Charge-Transfer
630 Excited-State Lifetime. *J. Phys. Chem. Lett.* **2018**, *9*, 459–463.
- 631 (80) Dixon, I. M.; Alary, F.; Boggio-Pasqua, M.; Heully, J.-L. The (N₄C₂)₂- Donor Set as
632 Promising Motif for Bis(Tridentate) Iron(II) Photoactive Compounds. *Inorg. Chem.* **2013**,
633 *52*, 13369–13374.
- 634 (81) Dixon, I. M.; Alary, F.; Boggio-Pasqua, M.; Heully, J.-L. Reversing the Relative ³MLCT-
635 ³MC Order in Fe(II) Complexes Using Cyclometallating Ligands: A Computational Study
636 Aiming at Luminescent Fe(II) Complexes. *Dalton Trans.* **2015**, *44*, 13498–13503.
- 637 (82) Dierks, P.; Kruse, A.; Bokareva, O. S.; Al-Marri, M. J.; Kalmbach, J.; Baltrun, M.; Neuba,
638 A.; Schoch, R.; Hohloch, S.; Heinze, K.; Seitz, M.; Kühn, O.; Lochbrunner, S.; Bauer, M.

- 639 Distinct Photodynamics of κ -N and κ -C Pseudoisomeric Iron(II) Complexes. *Chem.*
640 *Commun.* **2021**, *57*, 6640–6643.
- 641 (83) Leis, W.; Argüello Cordero, M. A.; Lochbrunner, S.; Schubert, H.; Berkefeld, A. A
642 Photoreactive Iron(II) Complex Luminophore. *J. Am. Chem. Soc.* **2022**, *144*, 1169–1173.
- 643 (84) Epstein, L. M. Moessbauer Isomer Shifts of Ferrous Phenanthroline and Related
644 Complexes. *J. Chem. Phys.* **1964**, *40*, 435–439.
- 645 (85) Reiff, W. M.; Baker, W. A., Jr.; Erickson, N. E. Binuclear, Oxygen-Bridged Complexes of
646 Iron(III). New Iron(III)-2,2',2"-Terpyridine Complexes. *J. Amer. Chem. Soc.* **1968**, *90*,
647 4794–4800.
- 648 (86) Chábera, P.; Liu, Y.; Prakash, O.; Thyraug, E.; Nahhas, A. E.; Honarfar, A.; Essén, S.;
649 Fredin, L. A.; Harlang, T. C. B.; Kjær, K. S.; Handrup, K.; Ericson, F.; Tatsuno, H.;
650 Morgan, K.; Schnadt, J.; Häggström, L.; Ericsson, T.; Sobkowiak, A.; Lidin, S.; Huang,
651 P.; Styring, S.; Uhlig, J.; Bendix, J.; Lomoth, R.; Sundström, V.; Persson, P.; Wärnmark,
652 K. A Low-Spin Fe(III) Complex With 100-Ps Ligand-to-Metal Charge Transfer
653 Photoluminescence. *Nature* **2017**, *543*, 695.
- 654 (87) Kjær, K. S.; Kaul, N.; Prakash, O.; Chábera, P.; Rosemann, N. W.; Honarfar, A.;
655 Gordivska, O.; Fredin, L. A.; Bergquist, K.-E.; Häggström, L.; Ericsson, T.; Lindh, L.;
656 Yartsev, A.; Styring, S.; Huang, P.; Uhlig, J.; Bendix, J.; Strand, D.; Sundström, V.;
657 Persson, P.; Lomoth, R.; Wärnmark, K. Luminescence and Reactivity of a Charge-
658 Transfer Excited Iron Complex with Nanosecond Lifetime. *Science* **2019**, *363*, 249.
- 659 (88) Betley, T. A.; Qian, B. A.; Peters, J. C. Group VIII Coordination Chemistry of a Pincer-
660 Type Bis(8-Quinolinyl)Amido Ligand. *Inorg. Chem.* **2008**, *47*, 11570–11582.
- 661 (89) Basch, H.; Viste, A.; Gray, H. B. Molecular Orbital Theory for Octahedral and Tetrahedral
662 Metal Complexes. *J. Chem. Phys.* **1966**, *44*, 10–19.
- 663 (90) Braun, J. D.; Lozada, I. B.; Kolodziej, C.; Burda, C.; Newman, K. M. E.; van Lierop, J.;
664 Davis, R. L.; Herbert, D. E. Iron(II) Coordination Complexes with Panchromatic
665 Absorption and Nanosecond Charge-Transfer Excited State Lifetimes. *Nat. Chem.* **2019**,
666 *11*, 1144–1150.
- 667 (91) Mukherjee, S.; Torres, D. E.; Jakubikova, E. HOMO Inversion as a Strategy for Improving
668 the Light-Absorption Properties of Fe(II) Chromophores. *Chem. Sci.* **2017**, *8*, 8115–8126.
- 669 (92) Braun, J. D.; Lozada, I. B.; Herbert, D. E. In Pursuit of Panchromatic Absorption in Metal
670 Coordination Complexes: Experimental Delineation of the HOMO Inversion Model Using
671 Pseudo-Octahedral Complexes of Diarylamido Ligands. *Inorg. Chem.* **2020**, *59*, 17746–
672 17757.
- 673 (93) Larsen, C. B.; Braun, J. D.; Lozada, I. B.; Kunnus, K.; Biasin, E.; Kolodziej, C.; Burda,
674 C.; Cordones, A. A.; Gaffney, K. J.; Herbert, D. E. Reduction of Electron Repulsion in
675 Highly Covalent Fe-Amido Complexes Counteracts the Impact of a Weak Ligand Field on
676 Excited-State Ordering. *J. Am. Chem. Soc.* **2021**, *143*, 20645–20656.
- 677 (94) Dixon, I. M.; Khan, S.; Alary, F.; Boggio-Pasqua, M.; Heully, J.-L. Probing the
678 Photophysical Capability of Mono and Bis(Cyclometallated) Fe(II) Polypyridine
679 Complexes Using Inexpensive Ground State DFT. *Dalton Trans.* **2014**, *43*, 15898–15905.
- 680 (95) Brown, A. M.; McCusker, C. E.; McCusker, J. K. Spectroelectrochemical Identification of
681 Charge-Transfer Excited States in Transition Metal-Based Polypyridyl Complexes. *Dalton*
682 *Trans.* **2014**, *43*, 17635–17646.

- 683 (96) Gaffney, K. J. Capturing Photochemical and Photophysical Transformations in Iron
684 Complexes with Ultrafast X-Ray Spectroscopy and Scattering. *Chem. Sci.* **2021**, *12*, 8010–
685 8025.
- 686 (97) Smeigh, A. L.; Creelman, M.; Mathies, R. A.; McCusker, J. K. Femtosecond Time-
687 Resolved Optical and Raman Spectroscopy of Photoinduced Spin Crossover: Temporal
688 Resolution of Low-to-High Spin Optical Switching. *J. Am. Chem. Soc.* **2008**, *130*, 14105–
689 14107.
- 690 (98) Sinha, N.; Jiménez, J.-R.; Pfund, B.; Prescimone, A.; Piguet, C.; Wenger, O. S. A Near-
691 Infrared-II Emissive Chromium(III) Complex. *Angew. Chem., Int. Ed.* **2021**, *60*, 23722–
692 23728.
- 693 (99) Sinha, N.; Pfund, B.; Wegeberg, C.; Prescimone, A.; Wenger, O. S. Cobalt(III) Carbene
694 Complex with an Electronic Excited-State Structure Similar to Cyclometalated
695 Iridium(III) Compounds. *J. Am. Chem. Soc.* **2022**, *144*, 9859–9873.
- 696 (100) Lozada, I. B.; Braun, J. D.; Williams, J. A. G.; Herbert, D. E. Yellow-Emitting, Pseudo-
697 Octahedral Zinc Complexes of Benzannulated N^NO Pincer-Type Ligands. *Inorg. Chem.*
698 **2022**, *61*, 17568–17578.
- 699 (101) Constable, E. C.; Hartshorn, R. M.; Housecroft, C. E. 1,1'-Biisoquinolines-Neglected
700 Ligands in the Heterocyclic Diimine Family That Provoke Stereochemical Reflections.
701 *Molecules* **2021**, *26*, 1584.
702

703

704

705